The switch of thermal expansions triggered by itinerant electrons in isostructural metal trifluorides

Feiyu Qin,[1] Xiaoying Wang,[1] Lei Hu,[1*] NingJia,[2] Zhibin Gao,[1*] Umut Aydemir,[3,4] Jun Chen,[5*] Xiangdong Ding,[1] Jun Sun[1]

1 State Key Laboratory for Mechanical Behavior of Materials, Xi'an Jiaotong University, Xi'an 710049, China

2 School of Materials Science and Engineering, Nanyang Technological University, Singapore 639798, Singapore

3 Department of Chemistry, Koc University, Sariyer, Istanbul 34450, Turkey

4 Koç University Boron and Advanced Materials Application and Research Center (KUBAM), Sariyer, Istanbul, 34450, Turkey

5 Department of Physical Chemistry, University of Science and Technology Beijing, Beijing 100083, China.

Corresponding authors: leihu@xjtu.edu.cn (LH), zhibin.gao@xjtu.edu.cn (ZBG), junchen@ustb.edu.cn (JC)

Section 1: Experimental details

Synthesis. ScF_3 (99.9%) and TiF_3 (99.9%) in powder form were directly purchased from Sigma-Aldrich without further treatment.

Characterization. Laboratory X-ray diffraction measurements were performed on Bruker D8 Advance (40 kV, 40 mA). Synchrotron X-ray diffraction (SXRD) data were collected in the 11-ID-C beamline at Advanced Photo Sources (APS) of Argonne National Laboratory (ANL) with a wavelength of 0.117418 Å. Synchrotron X-ray total scattering data were also collected in the same beamline with a short sample-to-detector distance around 350 cm. Rietveld structure refinement was conducted by *Fullprof* software. The obtained 2D data were transformed into 1D data using Fit2D. G(r) functions were obtained by PDFgetX2.[1] Correction, background subtraction, and sample absorption were processed by PDFgetX2. Q resolution is 25 $Å^{-1}$. Structure refinement of the total scattering data was carried out on PDFgui.[2] Ultraviolet-visible (UV-vis) absorption spectra was collected on a V-650DS spectrometer (JASCO) using $BaSO_4$ as a reference.

Section 2: DFT calculation.

We have studied the phonon dispersion, and Grüneisen parameter (γ) as a function of phonon frequencies in cubic ScF_3 and TiF_3, based on DFT calculation as implemented in VASP,[3, 4] Since Ti has one more electron than Sc, we consider the doped ScF_3 would, to some extent, behave similar to TiF_3. The charge doping was simulated by adding electrons to the ScF_3 with a compensating uniform charge background of opposite sign. For the electron-doped ScF_3 calculations, the lattice volume is relaxed. The TiF_3 demonstrates a rhombohedral structure below 370 K, above which it transforms into a cubic one. To obtain the calculated phonon dispersion of cubic TiF_3, we fix the cubic symmetry and then relax lattice constants and atomic positions. To obtain an accurate atomic vibration, we have systematically studied the effect of exchange-correlation

functional on the lattice constant. Perdew, Burke, and Ernzherhof (PBE) almost always overestimates the lattice constants of solids, while LDA consistently underestimates the volume. Table S1 shows that meta-GGA (SCAN)[5] performs quite well. The deviation of the lattice constant of optimized ScF_3 is only 0.027% compared with the experimental data. Therefore, we applied this lattice constant as the equilibrium state without the doping effect. We set 600 eV as the electronic kinetic energy cutoff for the plane-wave basis. The optimization used the conjugate-gradient method, and the ionic Hellmann−Feynman forces in each atom and total energy were converged to 10^{-4} eV/Å and 10^{-8} eV in the structure optimization and force-constants calculation. In the phonon calculation, we adopted a 3 × 3 × 3 supercell and 3 × 3 × 3 k-mesh sampling to attain force constants. We computed the Grüneisen parameter by Phonopy with ±1% step deformation.[6]

Table S1. Lattice constants of ScF_3 from experimental results and calculations based on various exchange-correlation functionals.

Method	Lattice constant, a (Å)	Difference, δ (Å)†
SXRD refinement	4.01542	0
LDA	3.94643	-0.06899
LDA-D2	3.93036	-0.08505
LDA-D3	2.93412	-1.08130
LDA-optB86b	4.00013	-0.01529
LDA-optB88	4.00449	-0.01093
LDA-SCAN+rVV10	3.96927	-0.04615
LDA-DF2	4.05865	0.04323
PBE	4.06903	0.05361
PBE-D3	4.05762	0.04220
PBE-DF2	4.10194	0.08652
PBE-optB86B	4.04472	0.02930
PBE-optB88	4.04923	0.03381
PBEsol-D2	4.00747	-0.00794
PBEsol-D3	4.01767	0.00225
PBEsol-DF2	4.10194	0.08652
PBEsol-optB86b	4.04472	0.02930
PBEsol-optB88	4.04923	0.03381
PBEsol	4.02569	0.01027
PBE-SCAN+rVV10	**4.01514**	**-0.00027**

† The difference δ is defined by $\delta = a_{Exp} - a_{Calc}$.

Section 3: Synchrotron X-ray diffraction

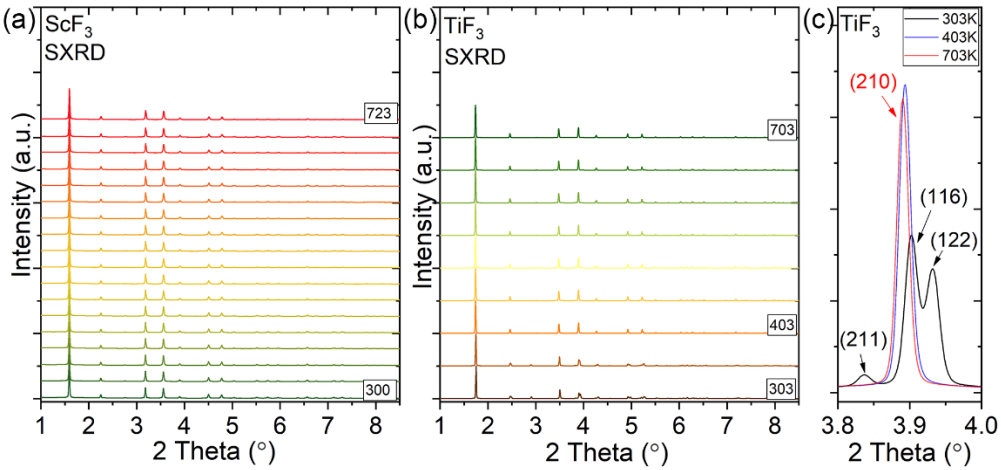

Figure S1. SXRD patterns of (a) ScF_3 and (b) TiF_3, (c) the enlarged 2-theta region (3.8° to 4.0°) of (b) for a close check of the structure transition rhombohedral into cubic, in which the split peaks merge into (210) peak with increasing temperature. It should be noted that the temperature intervals for ScF_3 and TiF_3 are about 25 K and 50 K, respectively. The lowest and highest temperatures are marked in (a) and (b).

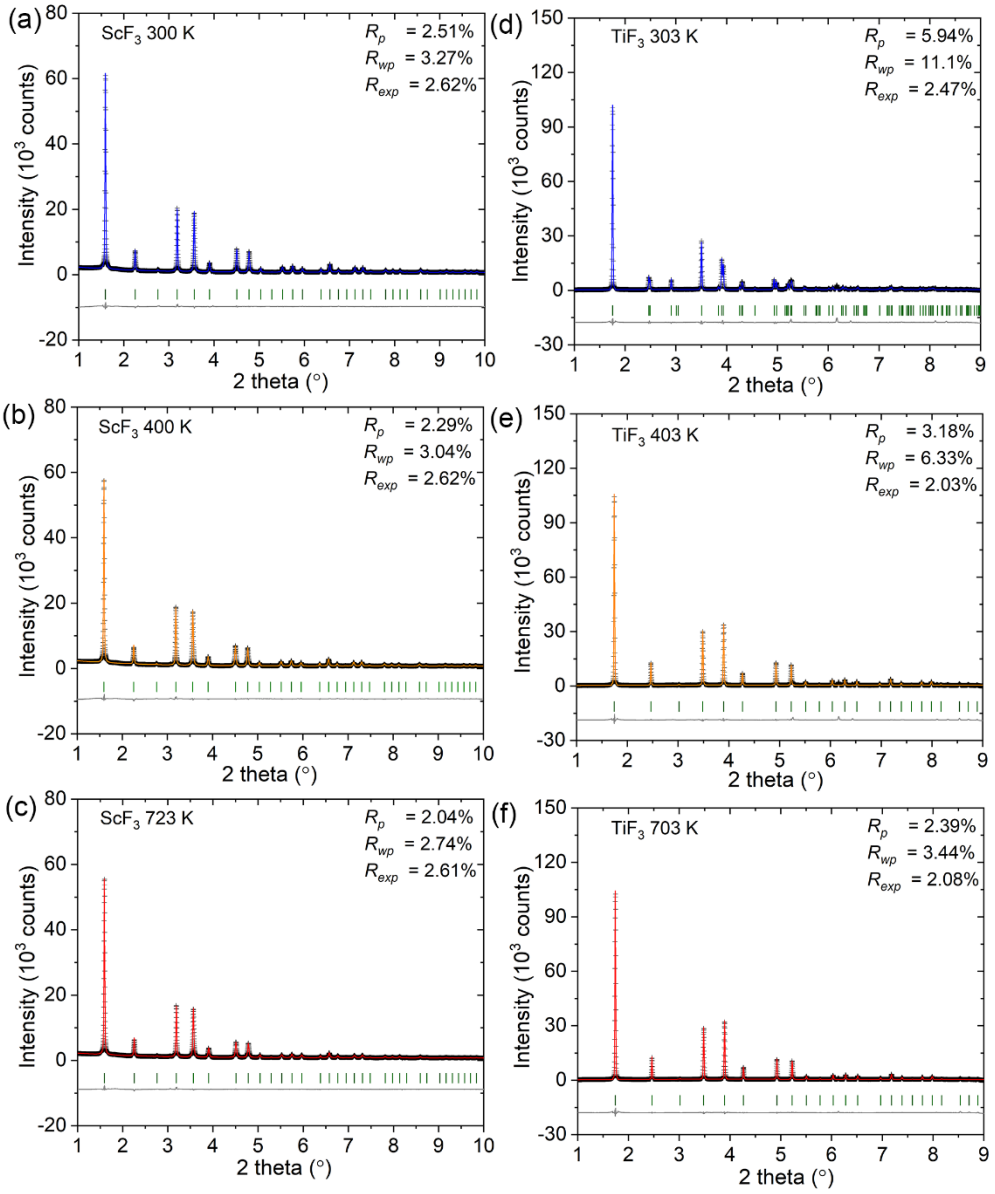

Figure S2. Rietveld structure refinement for SXRD patterns of ScF_3 at (a) 300 K, (b) 400 K and (c) 723 K, as well as refinement for SXRD patterns of TiF_3 at (d) 303 K, (e) 403 K and (f) 703 K. The goodness of fit, including R_p, R_{wp} and R_{exp} are listed in the upper-right corner of Figures. Note that TiF_3 demonstrates a rhombohedral structure at 303 K, whereas it transforms into a cubic one entirely at 403 K.

Section 4: The analysis of synchrotron X-ray pair distribution function (XPDF)

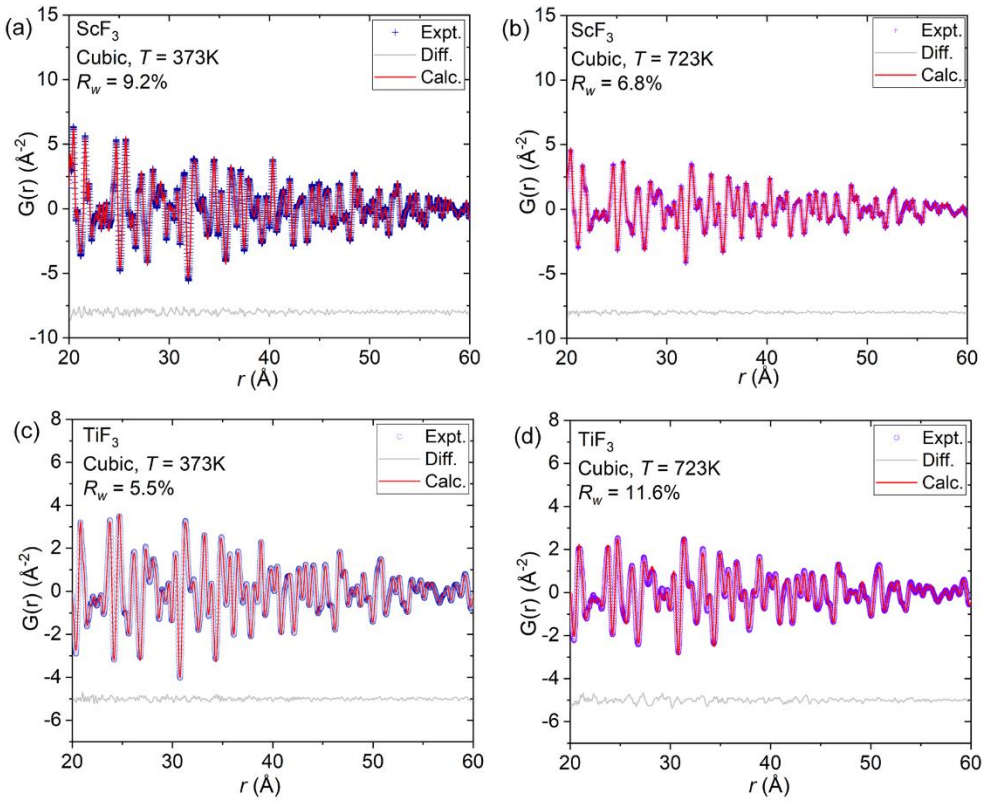

Figure S3. XPDF fit to G(r) functions for ScF_3 at (a) 373 K and (b) 723K. PDF fit to G(r) functions for TiF_3 at (c) 373 K and (d) 723 K. PDF fits here utilize long *r* range data from 20 Å to 60 Å, which aims for entirely revealing the global structure information. The fitted results, including lattice constants and atomic displacement parameters are presented in the main text. The smaller goodness of fit, R_w indicates the high degree of agreement between experimental data and cubic structures.

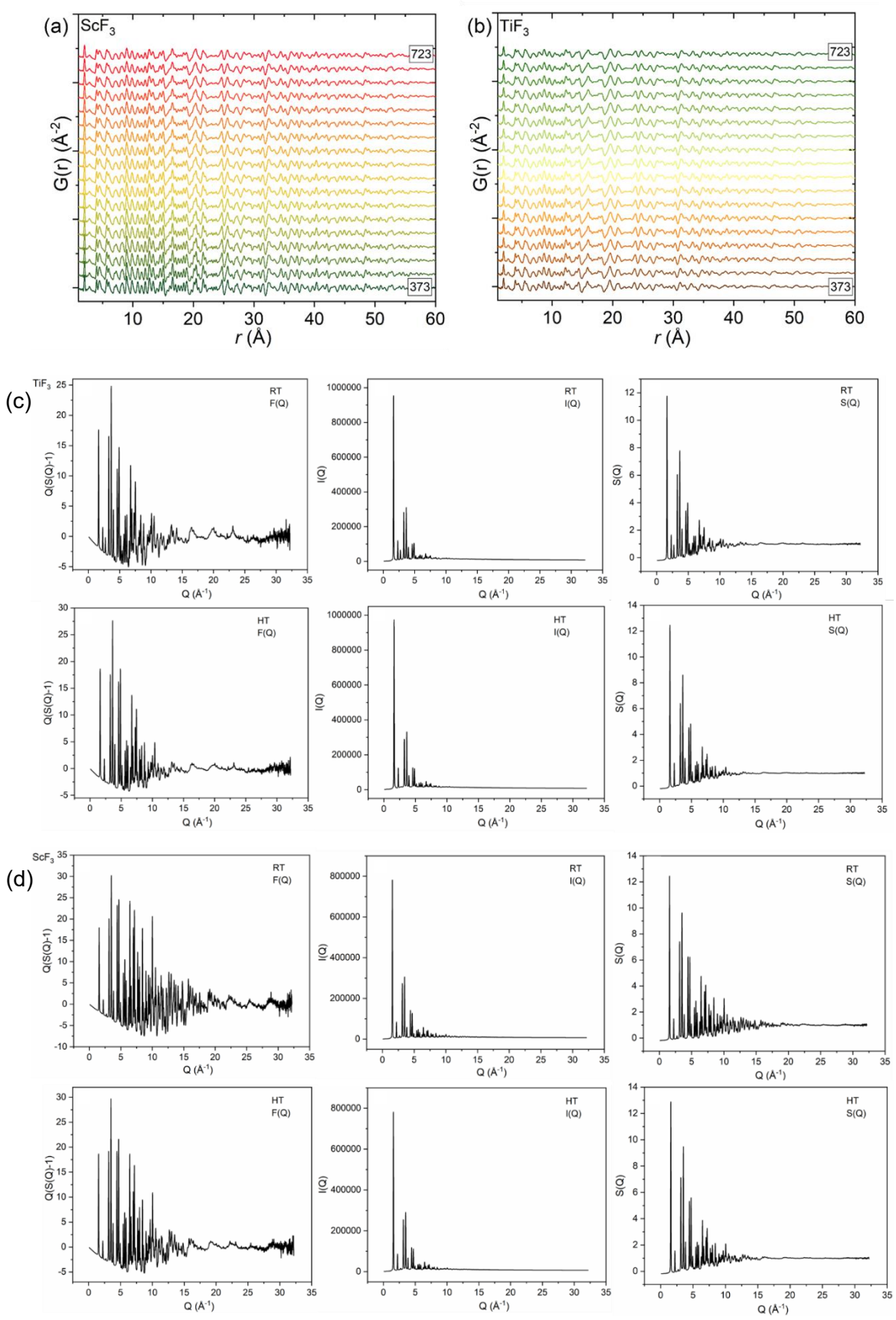

Figure S4. G(r) functions for (a) ScF_3 and (b) TiF_3 collected from 373 K to 723 K with the

interval of 25 K. I(Q), F(Q), and S(Q) functions of (c) ScF_3 and (d) TiF_3 at room temperature and high temperature.

Section 5: Magnetic measurement and Uv-vis absorbance spectrum

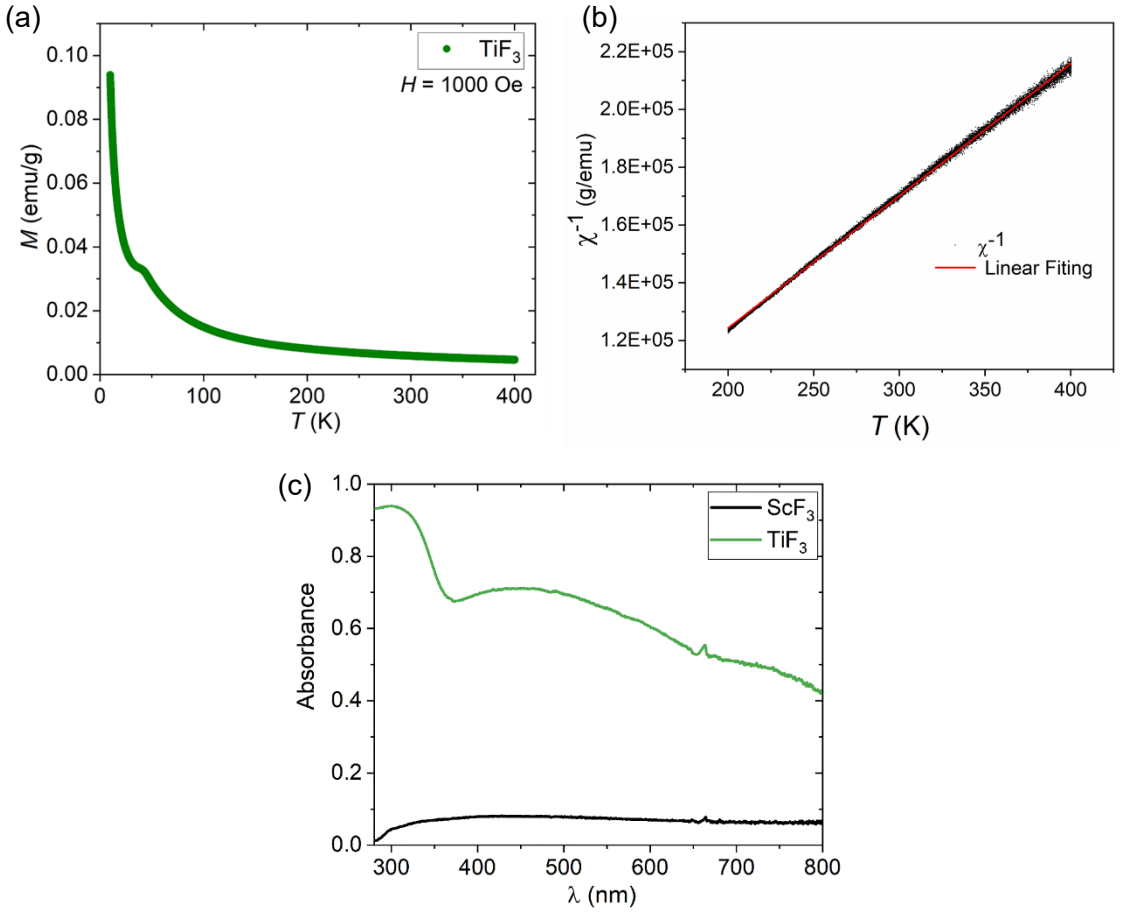

Figure S5. (a) Temperature dependence of MT curve of TiF_3. (b) Magnetic susceptibility of TiF_3 in the 200-400 K range. (c) Uv-vis absorption spectra of ScF_3 (black line) and TiF_3 (olive line). The low and high absorbance for ScF_3 and TiF_3 is in good agreement with their wide bandgap insulating and metallic features.

Section 6: The correlated Einstein model

The correlated Einstein model[7] is presented as follows:

$$\sigma^2 = \frac{\hbar^2}{2\mu k_B \Theta_E} \coth\left(\frac{\Theta_E}{2T}\right) + \sigma_{static}^2 \qquad \text{(S1)}$$

$$\omega_E = \frac{k_B \Theta_E}{\hbar} \qquad \text{(S2)}$$

$$f = \mu \omega_E^2 \qquad \text{(S3)}$$

where k_B is the Boltzmann's constant, $\hbar$ is the reduced Planck constant, μ is the reduced mass of a specific atomic pair, Θ_E is the Einstein temperature, ω_E is the Einstein frequency, and f is the force constant.

Table S6. Physical parameters used in the correlated Einstein model

Sample	Atomic pair	μ (g/mol)‡	Θ_E (K)	ω_E (THz)	f (eV/Å^2)
ScF_3	Sc···F	13.35	213.96	4.46	1.09
TiF_3	Ti···F	13.60	263.76	5.49	1.68

‡ The reduced mass μ is obtained by this equation, $m_1 * m_2/(m_1+m_2)$.

Section 7: The calculated phonon dispersions and electron density map

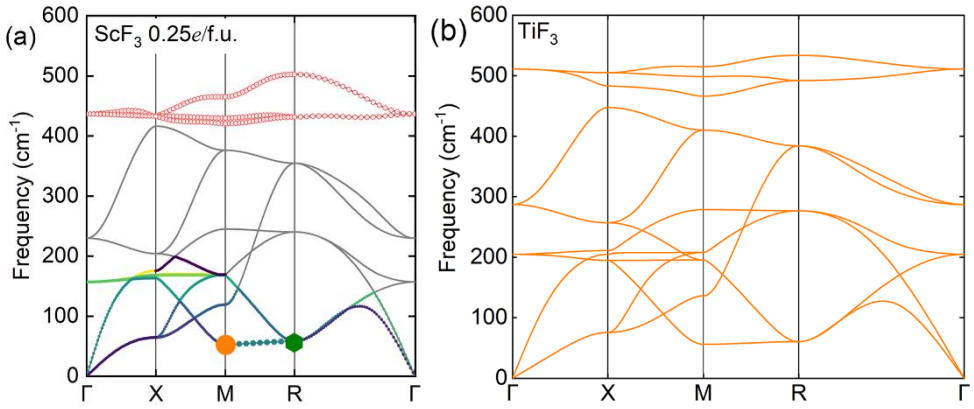

Figure S6. Phonon dispersions of (a) electron-doped cubic ScF_3 and (b) cubic TiF_3.

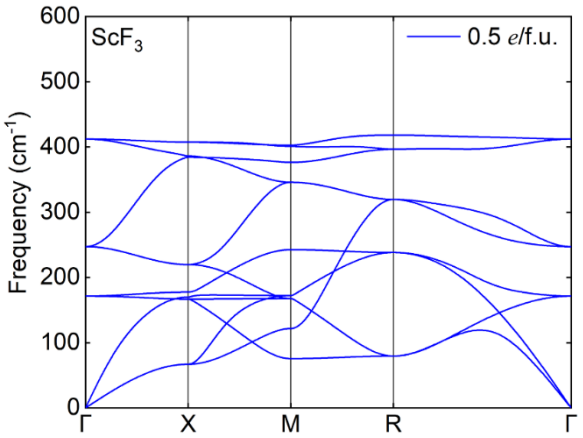

Figure S7. Phonon dispersion of electron-doped ScF_3 at 0.5 *e*/f.u concentration.

In order to explore the influence of itinerant electrons on thermal expansion, we utilize the electron localization function to examine chemical binding by DFT calculation.

We solve the Schrodinger equation by self-consistent calculation of electrons to calculate the electron wave function and charge density in the system's ground state. Then we can directly analyze the bond and action between atoms. We intercepted the miller indices hkl (0 0 1) plane through the origin to analyze the bonding information between atoms (Figure S8).

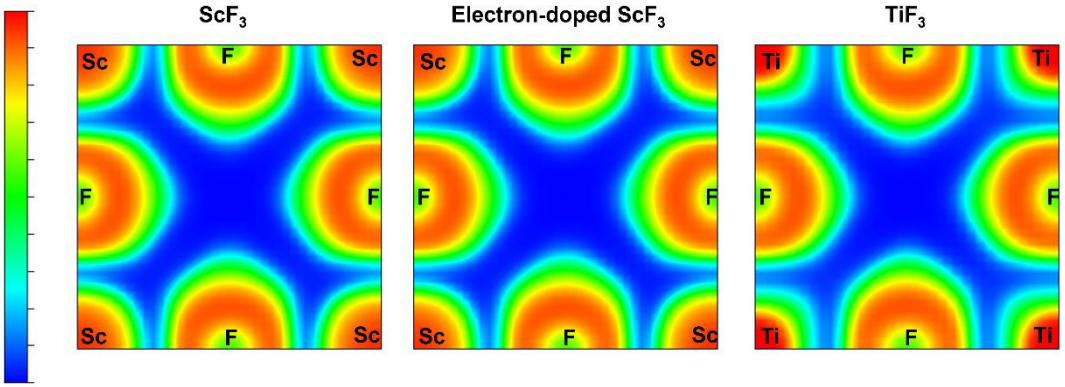

Figure S8. The electron density map of ScF_3, TiF_3, and electron-doped ScF_3.

The following equation calculated the chemical pressure P:

$$P = B(V_0\text{-}V)/V_0,$$

where B, V_0, and V represent the bulk modulus, the initial and the ultima lattice volume. The bulk modulus of ScF_3 and TiF_3 were obtained from an open-source online application.[8, 9] The lattice volumes V_0 and V were extracted from the XPDF data at 373 K and 723 K, respectively. Thus, the chemical pressures P of ScF_3 and TiF_3 are 0.102 GPa and -0.104 GPa, respectively.

References

1. X. Qiu, J. W. T., S. J. Billinge., PDFgetX2: a GUI-driven Program to Obtain the Pair Distribution Function from X-ray Powder Diffraction Data. *Journal of Applied Crystallography* **2004,** *37* (4), 678.
2. Farrow, C. L.; Juhas, P.; Liu, J. W.; Bryndin, D.; Bozin, E. S.; Bloch, J.; Proffen, T.; Billinge, S. J. L., PDFfit2 and PDFgui: computer programs for studying nanostructure in crystals. *J Phys-Condens Mat* **2007,** *19* (33), 335219.
3. Kresse, G.; Furthmuller, J., Efficiency of ab-initio total energy calculations for metals and semiconductors using a plane-wave basis set. *Comp Mater Sci* **1996,** *6* (1), 15-50.
4. Kresse, G.; Furthmuller, J., Efficient iterative schemes for ab initio total-energy calculations using a plane-wave basis set. *Physical Review B* **1996,** *54* (16), 11169-11186.
5. Sun, J. W.; Ruzsinszky, A.; Perdew, J. P., Strongly Constrained and Appropriately Normed Semilocal Density Functional. *Physical Review Letters* **2015,** *115* (3), 036402.
6. Togo, A.; Oba, F.; Tanaka, I., First-principles calculations of the ferroelastic transition between rutile-type and CaCl2-type SiO2 at high pressures. *Physical Review B* **2008,** *78* (13), 134106.
7. Purans, J.; Afify, N. D.; Dalba, G.; Grisenti, R.; De Panfilis, S.; Kuzmin, A.; Ozhogin, V. I.; Rocca, F.; Sanson, A.; Tiutiunnikov, S. I.; Fornasini, P., Isotopic effect in extended x-ray-absorption fine structure of germanium. *Phys Rev Lett* **2008,** *100* (5), 055901.
8. Gaillac, R.; Pullumbi, P.; Coudert, F. X., ELATE: an open-source online application for analysis and visualization of elastic tensors. *J Phys Condens Matter* **2016**, *28* (27), 275201.
9. https://progs.coudert.name/elate